

Kinetic energy and condensate fraction of superfluid ⁴He

V. F. Sears

Atomic Energy of Canada Limited, Chalk River, Ontario K0J 1J0, Canada

(Received 20 June 1983)

A new method for the experimental determination of the condensate fraction, n_0 , of superfluid ⁴He is presented. This method, which depends on the temperature variation of the average kinetic energy per atom, is applied to available neutron and x-ray data and yields values of n_0 that are consistent with those obtained from two previous methods. An analysis of the n_0 results from all methods gives the value $n_0 = (13.3 \pm 1.2)\%$ at $T=0$. This value is in excellent agreement with the value obtained recently by Campbell from the observed surface tension but is slightly higher than most theoretical estimates. The temperature variation of n_0 near the λ point, $T_\lambda = 2.17$ K, is consistent with the expected form $n_0 \approx (T_\lambda - T)^{2\beta}$ and the critical exponent is estimated to be $2\beta = 0.5 \pm 0.2$.

I. INTRODUCTION

The unique properties of superfluid ⁴He are believed¹⁻⁴ to result from a Bose-Einstein condensation which is characterized by the macroscopic occupation of the zero-momentum state. The fraction of atoms in this state n_0 is called the condensate fraction and recent theoretical calculations of n_0 at temperature $T=0$ give values for n_0 of^{5,6} 11.3% and⁷ 9.0% depending on the interatomic-force model.

The condensate fraction has been determined experimentally from both neutron inelastic scattering measurements at large momentum transfer^{8,9} and from the pair correlation functions obtained from neutron-diffraction¹⁰⁻¹² and x-ray-diffraction¹³ experiments. The results are mutually consistent and together yield⁹ a value $n_0 = 13.9 \pm 2.3\%$ at $T=0$ which is somewhat larger than the above theoretical values. Recently, Campbell¹⁴ has developed a method for evaluating n_0 in terms of the measured surface tension from which he estimates that $n_0 = 13\%$ at $T=0$ which is in excellent agreement with the value obtained from the other methods.

In the present paper we propose a new method for the experimental determination of the condensate fraction which depends on the temperature variation of the average atomic kinetic energy. The latter quantity can be obtained from any of three different kinds of neutron measurements: inelastic scattering, diffraction, or transmission. We apply the method to available data and find values of n_0 as a function of temperature that are in good agreement with those obtained in the above-mentioned work.⁸⁻¹⁴

II. NEUTRON SCATTERING AND THE CONDENSATE FRACTION

Figure 1 illustrates five methods for determining the condensate fraction of superfluid ⁴He from various kinds of neutron measurements. Methods I and II are existing methods which will be reviewed briefly below. Methods III-V, which depend on the average atomic kinetic energy K , are the new methods which will be described in the present paper and applied to available neutron and x-ray results.

Neutron inelastic scattering measurements using, for example, a triple-axis crystal spectrometer enable one to determine the dynamic structure factor $S(Q, \omega)$ as a function of the energy transfer $\hbar\omega$ for an arbitrary fixed value of the momentum transfer $\hbar Q$. Method I is based on the fact that in the large- Q limit the scattering is described asymptotically by the impulse approximation^{15,16} in which case $S(Q, \omega)$ is the Doppler spectrum characteristic of the momentum distribution¹⁷ $n(\vec{p})$ of the atoms in the initial state so that

$$pn(\vec{p}) = \lim_{Q \rightarrow \infty} -\frac{1}{2\pi} \left[\frac{\hbar Q}{m} \right]^2 \frac{\partial}{\partial \omega} S(Q, \omega). \quad (1)$$

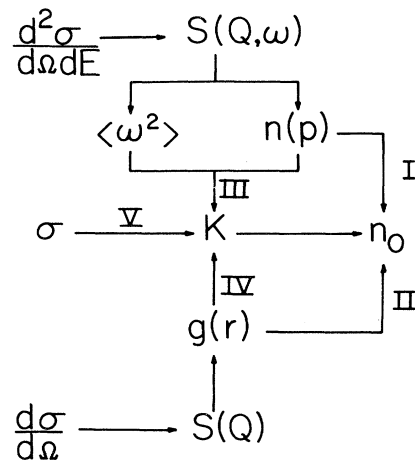


FIG. 1. Five methods for the determination of the condensate fraction n_0 of superfluid ⁴He from various kinds of neutron measurements.

Here m is the atomic mass and $p = (m/\hbar Q)(\omega - \omega_r)$ in which $\hbar\omega_r = (\hbar Q)^2/2m$ is the recoil energy. This relation has been used to determine momentum distributions for both liquid helium^{8,9,18,19} and liquid neon.²⁰

The momentum distribution of superfluid ^4He can be expressed in the form

$$n(\vec{p}) = n_0 \delta(\vec{p}) + (1 - n_0) n^*(\vec{p}), \quad (2)$$

where n_0 is the condensate fraction and $n^*(\vec{p})$ is the normalized momentum distribution function of the uncondensed atoms. The condensate peak in the measured $n(\vec{p})$ distributions is broadened by final-state interactions at the Q values for which data are presently available so that a distinct condensate peak cannot be resolved. Nevertheless, values of n_0 have been inferred from the observed temperature variation of $n(\vec{p})$ at small p .^{8,9}

Neutron-diffraction measurements²¹ enable one to determine the static structure factor $S(Q)$ and hence, by Fourier analysis, the pair correlation function $g(r)$. The approximate relation²²

$$g(r) - 1 = (1 - n_0)^2 [g^*(r) - 1], \quad (3)$$

when $r \geq 4.5 \text{ \AA}$ can then be used to obtain n_0 .¹⁰⁻¹³ This is referred to as method II in Fig. 1.

The final three methods depend on the average kinetic energy per atom,

$$K = \int \frac{(\hbar p)^2}{2m} n(\vec{p}) d\vec{p}, \quad (4)$$

which can be expressed with the help of (2) as

$$K = (1 - n_0) K^*, \quad (5)$$

where K^* is the average kinetic energy of the uncondensed atoms. As T increases from 0 to T_λ , the temperature variation of K is due partly to the depopulation of the zero-momentum state, which increases the factor $1 - n_0$, and partly to the creation of thermal excitations (phonons and rotons) which increases K^* . The contribution of the zero-point motion of the atoms to K will be essentially constant throughout the superfluid phase since the number density [Fig. 2(d)] changes by less than 1% below T_λ .

If, as in methods I and II, we assume that the depopulation of the zero-momentum state is the dominant effect then $K^*(T) \approx K(T_\lambda)$ and

$$n_0(T) \approx 1 - K(T)/K(T_\lambda). \quad (6)$$

However, strictly speaking, the right-hand side of (6) represents an upper limit on $n_0(T)$.

In method III the average kinetic energy is determined from the observed dynamic structure factor by means of the relation

$$K = \lim_{Q \rightarrow \infty} \frac{3\hbar}{4\omega_r} \int_{-\infty}^{\infty} (\omega - \omega_r)^2 S(Q, \omega) d\omega. \quad (7)$$

This relation can be obtained by substituting (1) into (4) or, alternatively, from the sum rules²³⁻²⁵ for $S(Q, \omega)$.

In method IV we use the energy equation,

$$U = K + V, \quad (8)$$

to determine K . Here U is the total internal energy, which can be obtained from thermodynamic measurements, and V is the potential energy which can be evaluated in terms of a model for the pair potential and the pair correlation function obtained from neutron- or x-ray-diffraction measurements.

Neutron-transmission measurements determine the total scattering cross section $\sigma(E_0)$ as a function of the incident-neutron energy E_0 . The asymptotic expression^{23,24}

$$\sigma(E_0) = \sigma(\infty) [1 + K/3AE_0 + O(E_0^{-3})], \quad (9)$$

in which A is the ratio of the nuclear mass over the neutron mass, can then be used to determine K from neutron-transmission measurements at large E_0 . This is the basis for method V.

Methods III and IV are applied to the determination of n_0 in the present paper and compared with previous results from methods I and II. The available total-scattering-cross-section data²⁶ are not at sufficiently high E_0 to permit a determination of n_0 using method V.

III. KINETIC ENERGY

We first consider the total internal energy, which is obtained by integrating the first law of thermodynamics,

$$U(T) = U(0) + \int_0^T C dT - \int_{v(0)}^{v(T)} p dv, \quad (10)$$

where C is the specific heat, p is the pressure, and v is the specific volume. Figure 2(a) shows the internal energy of liquid ^4He at saturated vapor pressure as a function of temperature calculated from (10) with²⁷ $U(0) = -7.14$

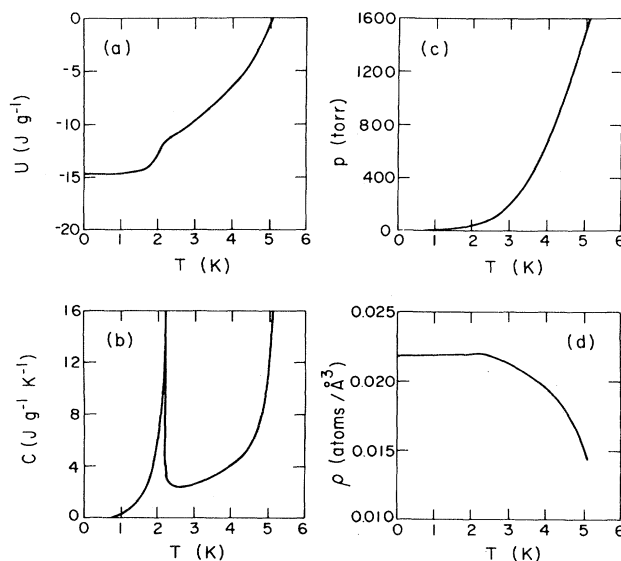


FIG. 2. (a) Internal energy of liquid ^4He at saturated vapor pressure calculated from (10) with the help of (b) the orthobaric specific heat (Refs. 28 and 29), (c) the saturated vapor pressure (Ref. 30), and (d) the number density (Ref. 31).

$\text{K}/\text{atom} = -14.83 \text{ J/g}$ and using the thermodynamic data shown in Figs. 2(b)–2(d). The logarithmic singularity²⁹ in the specific heat in the region $|T - T_\lambda| \leq 0.02 \text{ K}$ was integrated analytically. The temperature variation of $U(T)$ is due almost entirely to the specific-heat term in (10). The thermal-expansion term is largest at temperatures near the critical point (5.2 K) but even here it amounts to only 3% of the specific-heat term.

The potential energy can be calculated from the cluster expansion

$$V = V_2 + V_3 + \dots, \quad (11)$$

where V_n denotes the contribution from n -body forces. In particular,

$$V_2 = 2\pi\rho \int_0^\infty \phi(r)g(r)r^2 dr, \quad (12)$$

in which ρ is the number density, $\phi(r)$ is the pair potential, and $g(r)$ is the pair correlation function. In liquid ${}^4\text{He}$ the V_3 term represents a small correction, less than 7% of V_2 , and the four-body and higher-order terms in (11) are presumably negligible.

The HFDHE2 (Hartree-Fock dispersion) potential of Aziz *et al.*³² provides the most accurate representation of $\phi(r)$ that is available at this time. This potential, which is shown in Fig. 3(a), has been chosen such that it fits the results of self-consistent Hartree-Fock calculations at small r and leads to agreement with the gas-phase thermodynamic and transport properties within the experimental error. The potential so obtained is then found to give an accurate prediction of the He-He differential scattering cross sections measured in atomic-beam experiments. Finally, the pair correlation function of liquid ${}^4\text{He}$ calculated⁷ at $T=0$ using the Green-function Monte Carlo (GFMC) method on the basis of the HFDHE2 potential

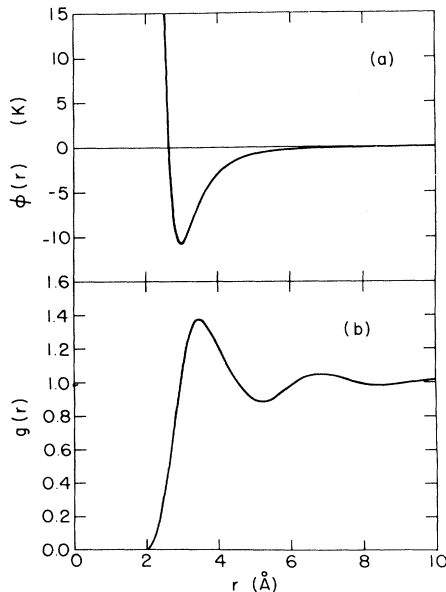


FIG. 3. (a) HFDHE2 potential for ${}^4\text{He}$ (Ref. 32), and (b) the pair correlation function for liquid ${}^4\text{He}$ at $T=1.00 \text{ K}$ obtained from neutron-diffraction measurements (Ref. 21).

agrees to within 1% with that obtained by neutron-diffraction measurements²¹ at $T=1.00 \text{ K}$ [Fig. 3(b)].

The values of V_2 calculated from (12) using the measured values³¹ of ρ , the HFDHE2 model³² for $\phi(r)$, and the neutron-^{12,21} and x-ray-diffraction^{33,34} results for $g(r)$ are listed in Table I. The small correction V_3 for three-body forces was interpolated at each density from values calculated⁷ using the GFMC method on the basis of the Axilrod-Teller three-body potential. These values of V_2 and V_3 , together with the value of the total internal energy U calculated from thermodynamics as described earlier, were then used in (8) to obtain the values of the kinetic energy K that are listed in Table I.

The kinetic energy can also be obtained from the virial theorem,³⁵

$$p = \frac{2}{3}\rho \left[K - \pi\rho \int_0^\infty \frac{d\phi(r)}{dr} g(r)r^3 dr \right]. \quad (13)$$

However, values of K obtained from this equation are very sensitive to experimental uncertainties in $g(r)$ at $r \approx 2.0 \text{ \AA}$ where $g(r) \rightarrow 0$ and $d\phi(r)/dr$ is very large (Fig. 3). For example, a variation of $g(r)$ by ± 0.005 for $r \leq 2.3 \text{ \AA}$ pro-

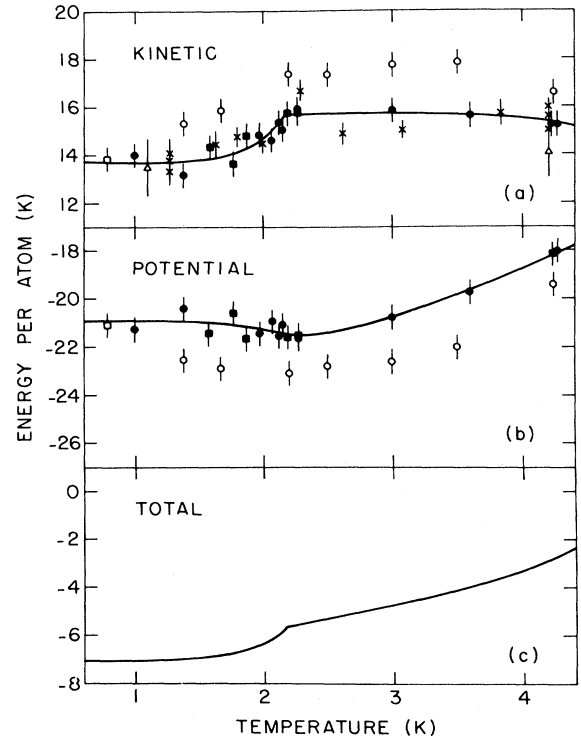


FIG. 4. (a) Kinetic energy K , (b) potential energy V_2 , and (c) total internal energy U , for liquid ${}^4\text{He}$ at saturated vapor pressure as a function of temperature calculated as described in the text. Solid symbols are values calculated using neutron-diffraction results for $g(r)$ (circles from Ref. 21 and squares from Ref. 12) and the open symbols using x-ray-diffraction results (circles from Ref. 34 and the square from Ref. 33). We also include values of the kinetic energy obtained directly from neutron inelastic scattering measurements (crosses from Ref. 36 and triangles from Ref. 37).

TABLE I. Kinetic and potential contributions to the internal energy of liquid ${}^4\text{He}$ in units of K/atom calculated as described in the text.

$g(r)$	T	U	=	K	+	V_2	+	V_3
Ref. 21 (neutron)	1.00	-7.13		14.00		-21.29		0.15
	1.38	-7.07		13.16		-20.38		0.15
	1.97	-6.45		14.82		-21.43		0.15
	2.07	-6.18		14.62		-20.95		0.15
	2.12	-6.00		15.38		-21.53		0.15
	2.15	-5.87		15.06		-21.09		0.15
	2.27	-5.58		15.93		-21.66		0.15
	3.00	-4.74		15.85		-20.74		0.14
	3.60	-3.93		15.63		-19.68		0.12
4.27	-2.70		15.23		-18.03		0.09	
Ref. 12 (neutron)	1.59	-6.69		14.35		-21.46		0.15
	1.77	-6.79		13.67		-20.61		0.15
	1.87	-6.64		14.86		-21.65		0.15
	2.19	-5.71		15.75		-21.61		0.15
	2.27	-5.58		15.75		-21.48		0.15
	4.23	-2.79		15.27		-18.15		0.10
Ref. 33 (x ray)	0.79	-7.14		13.85		-21.14		0.15
Ref. 34 (x ray)	1.38	-7.07		15.33		-22.55		0.15
	1.67	-6.89		15.85		-22.90		0.15
	2.20	-5.69		17.38		-23.22		0.15
	2.50	-5.31		17.35		-22.80		0.15
	3.00	-4.74		17.73		-22.61		0.14
	3.50	-4.08		17.84		-22.04		0.13
	4.24	-2.76		16.58		-19.43		0.10

duces a corresponding variation in the value of K obtained from the virial theorem (13) of ± 1.38 K/atom; but for the energy equation (8) the variation in K is only ± 0.22 K/atom.

The results listed in Table I are also shown in Fig. 4. The solid symbols are the values calculated using neutron-diffraction results for $g(r)$ (circles from Ref. 21 and squares from Ref. 12) and the open symbols using x-ray-diffraction results (circles from Ref. 34 and the square from Ref. 33). We also include values of the kinetic energy obtained directly from neutron inelastic scattering measurements, i.e., method III (crosses from Ref. 36 and triangles from Ref. 37).

The values of V_2 calculated using the x-ray results of Robkoff and Hallock³⁴ for $g(r)$, which are represented by the open circles in Fig. 4(b), are systematically lower than the other values by about 1–2 K/atom and the corresponding values of K [Fig. 4(a)] are higher by the same amount. This discrepancy of about 7% in V_2 is due to the fact that the threshold below which $g(r) \approx 0$ occurs in the neutron results^{12,21} at $r \approx 2.0$ Å and in the x-ray results³⁴ at a slightly higher value of $r \approx 2.2$ Å. One would expect the neutron results for $g(r)$ to be more accurate than the x-ray results at small r since $S(Q)$ was measured out to $Q = 10.8$ Å⁻¹ in the neutron-diffraction measurements but only out to $Q = 5.1$ Å⁻¹ in the x-ray-diffraction measure-

ments because of the rapid decrease in the atomic form factor at large Q . This assertion is borne out by the fact that the values of K in Fig. 4(a) calculated by method IV using the neutron-diffraction results (solid circles and squares) are in excellent agreement with the values calculated by method III (crosses and triangles).

Uncertainties in the pair potential can also produce systematic errors in V_2 and, hence, in K . For example, if we use the MS12G6 (modified Maitland-Smith) potential, which³² provides a fit to the gas-phase thermodynamic and transport properties that is almost as good as is obtained with the HFDHE2 potential, we find that the calculated values of K are increased by an amount 0.64 ± 0.04 K/atom that is essentially independent of temperature. Such a shift in the K values will, in first approximation, not affect the values of n_0 calculated from (6).

The above considerations of the sensitivity of V_2 to possible uncertainties in $\phi(r)$ and $g(r)$ therefore lead us to conclude that the calculated values of V_2 and, hence of K , are accurate to within about ± 0.5 K. The statistical fluctuations of the data points in Fig. 4 are consistent with this estimate.

We have drawn smooth curves through the data points in Figs. 4(a) and 4(b) as a guide to the eye, ignoring the open circles for reasons discussed above. Consider first the potential energy in Fig. 4(b). It is evident from (12)

TABLE II. Comparison of the present experimentally determined kinetic and potential energies of liquid ${}^4\text{He}$ (in units of K/atom) with theoretical calculations at $T=0$.

Authors (year)	Reference	Potential	Method	U	$= K$	$+ V_2$	$+ V_3$
London (1954)	1	Hard-sphere	Free-volume		14.6		
McMillan (1965)	38	Lennard-Jones	Variational	-5.66	14.6	-19.82	0
Schiff and Verlet (1967)	39	Lennard-Jones	Variational	-5.73	13.73	-19.46	0
Massey and Woo (1967)	40	Lennard-Jones	Variational	-6.02	14.30	-20.32	0
Gaglione <i>et al.</i> (1980)	41	Lennard-Jones	Variational	-6.10	13.96	-20.06	0
Whitlock <i>et al.</i> (1979)	5	Lennard-Jones	GFMC	-6.85	13.62	-20.47	0
Kalos <i>et al.</i> (1981)	7	Lennard-Jones	GFMC	-6.69	13.62	-20.47	0.16
Usmani <i>et al.</i> (1982)	42	HFDHE2	Variational	-6.96	14.77	-21.73	0
Kalos <i>et al.</i> (1981)	7	HFDHE2	GFMC	-6.97	14.47	-21.59	0.15
Present work ($T=1.00$ K)		HFDHE2	Experimental	-7.13	14.00	-21.29	0.15

that the temperature variation of V_2 is due to the corresponding variations in ρ and $g(r)$. As T increases from 0 to $T_\lambda=2.17$ K, V_2 decreases by about 3% while ρ increases by only 0.7%. In this region the variation of V_2 is due mainly to $g(r)$. However, as T increases from T_λ to the boiling point (4.2 K), $|V_2|$ and ρ both decrease by 14%. Here, ρ is mainly responsible for the temperature variation of V_2 .

Now consider the kinetic energy in Fig. 4(a) where it is seen that as T increases from 0 to T_λ , K increases by 15%, of which two thirds comes from the change in U and one-third from the change in V_2 . Since the number density ρ , and hence the zero-point energy, is essentially constant in this region, the temperature variation in K arises from the depopulation of the zero-momentum state and also, to some extent, from the creation of thermal excitations among the uncondensed atoms. On the other hand, as T increases from T_λ to 4.2 K, the kinetic energy is almost constant and, in fact, there is an indication of a slight decrease of about 3%. Here the decrease in the zero-point energy from the 14% decrease in ρ cancels the tendency for K to increase as a result of the creation of further thermal excitations.

Finally, Table II shows a comparison of the kinetic and potential energies which we have determined by method IV at $T=1.00$ K with the results of various theoretical calculations at $T=0$. Since the HFDHE2 potential provides a more accurate representation of the ${}^4\text{He}$ pair potential than does the Lennard-Jones potential,³² the variational calculations of Usmani *et al.*⁴² and the GFMC calculations of Kalos *et al.*⁷ are the most relevant for comparison with our present results. Since the accuracy of our values of V_2 and, hence of K , was estimated above to be ± 0.5 K, the agreement with the theoretical values can be regarded as satisfactory.

IV. CONDENSATE FRACTION

In Table III we list the values of n_0 obtained in earlier work using methods I (Refs. 8 and 9) and II (Refs. 10–13). We also give the values obtained in the present work from (6) with the kinetic energy determined by methods III (Refs. 36 and 37) and IV (Table I). In applying the relation (6), the value of K at T_λ was taken to be 15.75 K/atom with the following exception. The K values corresponding to the open circles in Fig. 4 are displaced

relative to the other values for reasons discussed in the last section. To compensate for this fact the value $K(T_\lambda)=17.38$ K/atom was assumed (see Table I).

The results in Table III are also shown in Fig. 5 where it is seen that all four methods yield values of n_0 that are mutually consistent within the present uncertainty. The smooth curve in Fig. 5 is the result of a least-squares fit to the expression

$$n_0(T) = n_0(0)[1 - (T/T_\lambda)^\alpha], \quad (14)$$

which gives $n_0(0)=13.3\pm 1.2\%$ and $\alpha=4.7\pm 1.2$. These are consistent with the previous values⁹ $n_0(0)=13.9\pm 2.3\%$ and $\alpha=3.6\pm 1.4$ which were obtained by fitting (14) to the results of methods I and II alone.

The analytic form of Eq. (14) is true for an ideal Bose-Einstein gas¹ for which $n_0(0)=100\%$ and $\alpha=\frac{3}{2}$. It has no real justification for liquid ${}^4\text{He}$; we simply regard it as a convenient way of parametrizing the data and of es-

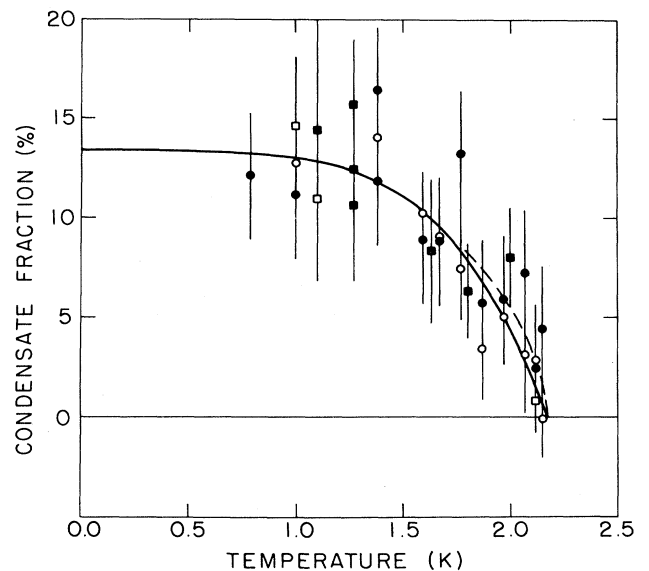


FIG. 5. Condensate fraction of superfluid ${}^4\text{He}$ as a function of temperature. Data points are those listed in Table III: method I (open squares), method II (open circles), method III (solid squares), and method IV (solid circles). Smooth curve is a least-squares fit to Eq. (14) and dashed curve the same to Eq. (16).

TABLE III. Experimentally determined values of the condensate fraction of superfluid ^4He . Values for method I are from Refs. 8 and 9, and those for method II are from Refs. 10–13. Values for methods III and IV are obtained in the present work as described in the text.

T (K)	n_0 (%)				
	I	II	III	IV	
0.79				12.1±3.2	
1.00	14.6±3.5	12.7±2.0		11.1±3.2	
1.10	10.9±2.7		14.4±7.6		
1.27			10.6±3.8		
1.27			15.7±3.2		
1.27			12.4±1.9		
1.38		14.0±3.4		16.4±3.2	
1.38				11.8±3.2	
1.59		10.2±2.1		8.9±3.2	
1.63			8.3±3.6		
1.67		9.0±3.0		8.8±3.2	
1.77		7.4±2.5		13.2±3.2	
1.80			6.3±2.4		
1.87		3.4±2.6		5.7±3.2	
1.97		5.0±2.4		5.9±3.2	
2.00			8.0±2.5		
2.07		3.1±2.9		7.3±3.2	
2.12	0.8±0.6	2.8±2.9		2.4±3.2	
2.15		-0.1±1.9		4.4±3.2	

timating the value of n_0 at $T=0$. In fact, the asymptotic behavior of n_0 as $T \rightarrow 0$ is given by⁴³

$$n_0(T) = n_0(0)[1 - (T/T_0)^2], \quad (15)$$

where $(k_B T_0)^2 = 12\hbar^3 c \rho / m$ in which k_B is Boltzmann's constant and c is the velocity of sound at $T=0$. With² $c=239$ m/s we find that $T_0=7.62$ K. Hence, $n_0(T)$ changes by less than 2% below $T=1$ K so that the accuracy of our estimate of $n_0(0)$ is not limited by the degree of validity of Eq. (14).

As $T \rightarrow T_\lambda$ from below, the condensate fraction is expected⁴⁴ to have the form

$$n_0(T) \simeq (T_\lambda - T)^{2\beta}, \quad (16)$$

where the exponent 2β is at present unknown. A least-squares fit of (16) to the n_0 values in Table III for $T \geq 1.80$ K gives the value $2\beta=0.5 \pm 0.2$ and is represented by the dashed curve in Fig. 5. Because of the large degree of scatter in the data, and the fact that the temperatures are not very close to T_λ , this estimate of 2β must, however, be regarded as tentative.

TABLE IV. Comparison of theoretical and experimental values of the condensate fraction of superfluid ^4He at $T=0$.

Authors (year)	Reference	Method	n_0 (%)
Theoretical			
Penrose and Onsager (1956)	45	Variational	8
McMillan (1965)	38	Variational	11
Schiff and Verlet (1967)	39	Variational	10.5
Francis <i>et al.</i> (1970)	46	Variational	10.1
Ristig <i>et al.</i> (1975)	47	Variational	11.9
Lam and Ristig (1979)	6	Variational	11.3
Kalos <i>et al.</i> (1974)	48	GFMC	9.5
Whitlock <i>et al.</i> (1979)	5	GFMC	11.3
Kalos <i>et al.</i> (1981)	7	GFMC	9.0
Experimental			
Campbell (1983)	14	Surface tension	13
Present work	8 and 9	I	12.8±1.8
	10–13	II	13.9±2.7
	Table III	III	13.5±2.6
	Table III	IV	12.2±4.5
		all	13.3±1.2

V. DISCUSSION

Table IV shows a comparison of the results of a number of theoretical calculations of the condensate fraction of superfluid ^4He at $T=0$ with the experimentally determined values. We include here the values of $n_0(0)$ determined by a least-squares fit of Eq. (14) to the results in Table III for each method separately as well as the fit to all the results. The experimentally determined values are in mutual agreement within the uncertainties but are somewhat higher than the theoretical values.

The best theoretical estimate of $n_0(0)$ is presumably the value 9.0% obtained recently by Kalos *et al.*⁷ using the ostensibly exact GFMC method together with the HFDHE2 model for the pair potential. The earlier theoretical values in Table IV used the less accurate Lennard-Jones potential and, in this respect, yielded values for n_0 that would be expected to be less reliable than that of Ref. 7. Nevertheless, the earlier theoretical calculations of n_0 mostly give values in the range of 10–12% that are more in agreement with the present experimental values.

The fundamental assumption in all the methods in Fig. 1 is that the temperature variation of $n(\vec{p})$, $g(r)$, and K in the superfluid phase is due primarily to the variation of n_0 and that the effect of any variation of $n^*(\vec{p})$, $g^*(r)$, and K^* is relatively less important and, hence, can be neglected in first approximation.⁴⁹ This assumption is clearly a potential source of systematic error in the experimental values of n_0 . However, the fact that methods I–IV yield values of n_0 that agree, not only with each other, but also with the value estimated by Campbell¹⁴ from surface-tension measurements, suggests that such systematic errors may be rather small. Further theoretical work, not

only on the *ab initio* calculation of n_0 , but also on the justification of the assumptions employed in the various experimental methods would, nevertheless, clearly be of considerable value.

The values of n_0 listed in Table III all refer to saturated vapor pressure. Recently, Wirth *et al.*⁵⁰ have studied the density dependence of the values of n_0 obtained by method II from x-ray-diffraction experiments. Contrary to expectation they find that changes in density of up to 14% produce no appreciable change in the condensate fraction. Fitting their results for all pressures to Eq. (14) they find the values $n_0(0)=11.2\pm 0.6\%$ and $\alpha=4.64\pm 0.48$ which agree reasonably well with those found in the present work (Sec. IV). Neutron inelastic scattering experiments are currently being carried out by Mook⁵¹ at Oak Ridge National Laboratory to determine n_0 by method I. His preliminary results yield values of n_0 at saturated vapor pressure that agree well with those in Table III. In contrast to Wirth *et al.*,⁵⁰ however, Mook finds a very strong decrease in n_0 with increasing pressure. Forthcoming neutron-scattering experiments⁵² on pressurized liquid ^4He at Chalk River Nuclear Laboratories will no doubt shed additional light on the important question of the density variation of the values of n_0 determined experimentally by the various methods listed in Fig. 1.

ACKNOWLEDGMENTS

The author is grateful to E. C. Svensson for helpful discussions and for his criticism of the manuscript, and also to P. A. Whitlock for communicating some unpublished kinetic and potential energy results from GFMC calculations.

¹F. London, *Superfluids* (Wiley, New York, 1954), Vol. 2.

²K. R. Atkins, *Liquid Helium* (Cambridge University Press, Cambridge, 1959).

³J. Wilks, *The Properties of Liquid and Solid Helium* (Oxford University Press, London, 1967).

⁴W. E. Keller, *Helium-3 and Helium-4* (Plenum, New York, 1969).

⁵P. A. Whitlock, D. M. Ceperley, G. V. Chester, and M. H. Kalos, *Phys. Rev. B* **19**, 5598 (1979).

⁶P. M. Lam and M. L. Ristig, *Phys. Rev. B* **20**, 1960 (1979).

⁷M. H. Kalos, M. A. Lee, P. A. Whitlock, and G. V. Chester, *Phys. Rev. B* **24**, 115 (1981); P. A. Whitlock (private communication).

⁸A. D. B. Woods and V. F. Sears, *Phys. Rev. Lett.* **39**, 415 (1977).

⁹V. F. Sears, E. C. Svensson, P. Martel, and A. D. B. Woods, *Phys. Rev. Lett.* **49**, 279 (1982).

¹⁰V. F. Sears and E. C. Svensson, *Phys. Rev. Lett.* **43**, 2009 (1979).

¹¹V. F. Sears and E. C. Svensson, *Int. J. Quantum Chem. Symp.* **14**, 715 (1980).

¹²V. F. Sears, E. C. Svensson, and A. F. Murray (unpublished).

¹³H. N. Robkoff, D. A. Ewen, and R. B. Hallock, *Phys. Rev. Lett.* **43**, 2006 (1979).

¹⁴L. J. Campbell, in *Proceedings of the Symposium on Quantum Liquids and Solids, Sanibel, Florida, 1983*, edited by E. D.

Adams and G. G. Ihas (AIP, New York, 1983); *Phys. Rev. B* **27**, 1913 (1983).

¹⁵P. C. Hohenberg and P. M. Platzman, *Phys. Rev.* **152**, 198 (1966).

¹⁶V. F. Sears, *Phys. Rev.* **185**, 200 (1969).

¹⁷Here \vec{p} denotes the wave vector of a ^4He atom so that the momentum is actually $\hbar\vec{p}$. The distribution function is normalized such that $\int n(\vec{p})d\vec{p}=1$.

¹⁸H. A. Mook, *Phys. Rev. Lett.* **32**, 1167 (1974).

¹⁹P. Martel, E. C. Svensson, A. D. B. Woods, V. F. Sears, and R. A. Cowley, *J. Low Temp. Phys.* **23**, 285 (1976).

²⁰V. F. Sears, *Can. J. Phys.* **59**, 555 (1981).

²¹E. C. Svensson, V. F. Sears, A. D. B. Woods, and P. Martel, *Phys. Rev. B* **21**, 3638 (1980); V. F. Sears, E. C. Svensson, A. D. B. Woods, and P. Martel, Atomic Energy of Canada Limited Report No. AECL-6779 (unpublished).

²²G. J. Hyland, G. Rowlands, and F. W. Cummings, *Phys. Lett.* **31A**, 465 (1970); F. W. Cummings, G. J. Hyland, and G. Rowlands, *Phys. Kondens. Mater.* **12**, 90 (1970).

²³G. Placzek, *Phys. Rev.* **86**, 377 (1952).

²⁴G. C. Wick, *Phys. Rev.* **94**, 1228 (1954).

²⁵A. Rahman, K. S. Singwi, and A. Sjölander, *Phys. Rev.* **126**, 986 (1962).

²⁶H. S. Sommers, J. G. Dash, and L. Goldstein, *Phys. Rev.* **97**, 855 (1955).

²⁷P. R. Roach, J. B. Ketterson, and C. W. Woo, *Phys. Rev. A* **2**,

- 543 (1970).
- ²⁸H. C. Kramers, J. D. Wasscher, and C. J. Gorter, *Physica* **18**, 329 (1952); R. W. Hill and O. V. Lounasmaa, *Philos. Mag.* **2**, 143 (1957).
- ²⁹M. J. Buckingham and W. M. Fairbank, *Prog. Low Temp. Phys.* **3**, 80 (1961).
- ³⁰H. Van Dijk and M. Durieux, *Physica* **24**, 920 (1958).
- ³¹E. C. Kerr and R. D. Taylor, *Ann. Phys. (N.Y.)* **26**, 292 (1964); R. D. McCarty, *J. Phys. Chem. Ref. Data* **2**, 923 (1973).
- ³²R. A. Aziz, V. P. S. Nain, J. S. Carley, W. L. Taylor, and G. T. McConville, *J. Chem. Phys.* **70**, 4330 (1979).
- ³³E. K. Achter and L. Meyer, *Phys. Rev.* **188**, 291 (1969).
- ³⁴H. N. Robkoff and R. B. Hallock, *Phys. Rev. B* **24**, 159 (1981).
- ³⁵J. O. Hirschfelder, C. F. Curtiss, and R. B. Bird, *Molecular Theory of Gases and Liquids* (Wiley, New York, 1954).
- ³⁶O. K. Harling, *Phys. Rev. Lett.* **24**, 1046 (1970); O. K. Harling, *Phys. Rev. A* **3**, 1073 (1971); A. G. Gibbs and O. K. Harling, *ibid.* **7**, 1748 (1973).
- ³⁷A. D. B. Woods and V. F. Sears, *J. Phys. C* **10**, L341 (1977).
- ³⁸W. L. McMillan, *Phys. Rev.* **138**, A442 (1965).
- ³⁹D. Schiff and L. Verlet, *Phys. Rev.* **160**, 208 (1967).
- ⁴⁰W. E. Massey and C. W. Woo, *Phys. Rev.* **164**, 256 (1967).
- ⁴¹G. Gaglione, G. L. Masserini, and L. Reatto, *Phys. Rev. B* **22**, 1237 (1980).
- ⁴²Q. N. Usmani, S. Fantoni, and V. R. Pandharipande, *Phys. Rev. B* **26**, 6123 (1982).
- ⁴³R. A. Ferrell, N. Menyhard, H. Schmidt, F. Schwabl, and P. Szeplafalussy, *Ann. Phys. (N.Y.)* **47**, 565 (1968); K. Kehr, *Z. Phys.* **221**, 291 (1969).
- ⁴⁴B. D. Josephson, *Phys. Lett.* **21**, 608 (1966).
- ⁴⁵O. Penrose and L. Onsager, *Phys. Rev.* **104**, 576 (1956).
- ⁴⁶W. P. Francis, G. V. Chester, and L. Reatto, *Phys. Rev. A* **1**, 86 (1970).
- ⁴⁷M. L. Ristig, P. M. Lam, and J. W. Clark, *Phys. Lett.* **55A**, 101 (1975).
- ⁴⁸M. H. Kalos, D. Levesque, and L. Verlet, *Phys. Rev. A* **9**, 2178 (1974).
- ⁴⁹In connection with method I, the temperature variation of $n^*(\vec{p})$ due to the p^{-2} singularity was taken into account in Ref. 9.
- ⁵⁰F. W. Wirth, D. A. Ewen, and R. B. Hallock, *Phys. Rev. B* **27**, 5530 (1983).
- ⁵¹H. A. Mook (private communication).
- ⁵²E. C. Svensson (private communication).